



Top-down controls on nutrient cycling and population dynamics in a model estuarine photoautotroph–heterotroph co-culture system

Qiang Zheng^{1,2} | Wenxin Lin^{1,2} | Yu Wang^{1,2} | Dapeng Xu^{1,2} | Yanting Liu^{1,2} | Nianzhi Jiao^{1,2}

¹State Key Laboratory for Marine Environmental Science, Institute of Marine Microbes and Ecospheres, College of Ocean and Earth Sciences, Xiamen University, Xiamen, People's Republic of China

²Fujian Key Laboratory of Marine Carbon Sequestration, Xiamen University, Xiamen, People's Republic of China

Correspondence

Qiang Zheng and Nianzhi Jiao, State Key Laboratory for Marine Environmental Science, Institute of Marine Microbes and Ecospheres, College of Ocean and Earth Sciences, Xiamen University, Xiamen 361102, People's Republic of China.
Email: zhengqiang@xmu.edu.cn; jiao@xmu.edu.cn

Funding information

National Key Research Programs, Grant/Award Number: 2018YFA0605800; National Natural Science Foundation of China, Grant/Award Number: 41776145, 41876150, 41861144018, 20720190095 and 2018J05072; Natural Science Foundation of Fujian Province

Abstract

Viral lysis and protistan grazing are thought to be the major processes leading to microbial mortality in aquatic environments and thus regulate community diversity and biogeochemical cycling characteristics. Here, we studied nutrient cycling and bacterial responses to cyanophage-mediated photoautotroph lysis and ciliate predation in a model *Synechococcus*–heterotroph co-culture system. Both viral lysis and *Euplotes* grazing facilitated the transformation of organic carbon from biomass to dissolved organic matter with conversion efficiencies of 20%–26%. The accumulation of ammonium after the addition of phages and ciliates suggested the importance of recycled NH_4^+ occurred in the interactions between *Synechococcus* growth and heterotrophic bacterial metabolism of photosynthate. The slower efficiency of P mineralization compared to N (primarily ammonium) indicated that P-containing organic matter was primarily integrated into bacterial biomass rather than being remineralized into inorganic phosphate under C-rich conditions. In the cyanophage addition treatment, both *Fluviicola* and *Alteromonas* exhibited rapid positive responses to *Synechococcus* lysing, while *Marivita* exhibited an apparent negative response. Further, the addition of *Euplotes* altered the incubation system from a *Synechococcus*-driven phycosphere to a ciliate-remodelled zoosphere that primarily constituted grazing-resistant bacteria and *Euplotes* symbionts. Top-down controls increased co-culture system diversity and resulted in a preference for free-living lifestyles of dominant populations, which was accompanied by the transfer of matter and energy. Our results indicate top-down control was particularly important for organic matter redistribution and inorganic nutrient regeneration between photoautotrophs and heterotrophs, and altered bacterial lifestyles. This study consequently sheds light on marine biogeochemical cycling and the interaction networks within these dynamic ecosystems.

KEYWORDS

ciliate grazing, heterotrophs, interactions, photoautotrophs, top-down control, viral lysis

1 | INTRODUCTION

Microorganisms play significant roles in the productivity and biogeochemical cycling in oceans (Azam et al., 1983; Jiao et al., 2010). Indeed, marine microorganisms are part of an interactive ecosystem, wherein their metabolic activities are mediated by bottom-up controls (e.g. nutrient bioavailability, light and temperature) and top-down controls (e.g. viral lysis and protistan grazing) (Chow et al., 2014; Hutchins & Fu, 2017; Morán et al., 2017; Suttle, 2007). The in situ standing stock of microorganisms is thereby determined by the balance between their growth and mortality rates (Pernthaler, 2005; Wommack & Colwell, 2000; Worden & Binder, 2003). Protistan grazing and viral-induced lysis are thought to be the major processes leading to microbial mortality in the ocean, and responsible for equivalent levels of bacterial decreases on average (Fischer et al., 2006; Fuhrman & Noble, 1995; Wommack & Colwell, 2000). Both of these mechanisms can accelerate nutrient cycling in environments, which is particularly important in oligotrophic open oceans (Billen et al., 1990; Boras et al., 2009; Caron & Goldman, 1988). However, the organic matter derived from the loss of microbial biomass from protistan grazing and viral lysis has different fates. The carbon from viral lysates enters the dissolved organic carbon (DOC)–bacteria–DOC loop (Bratbak et al., 1992; Talmy et al., 2019). In contrast, the carbon ingested by protozoa is transferred to higher trophic organisms (Boras et al., 2009; Dolan & Gallegos, 1991), while some of the organic carbon from sloppy grazing or egestion/excretion returns to the environment. Thus, bacteria, protists and viruses are connected within a complex ‘microbial loop’ (Azam et al., 1983).

Numerous studies have investigated how protistan grazing and viral lysis impact the structures of microbial communities (Baudoux et al., 2008; Chow et al., 2014; Sherr & Sherr, 2002; Weinbauer et al., 2007). For example, viruses can regulate microbial diversity via ‘kill the winner’ dynamics, wherein selective mortality is highly dependent on bacterial abundances (Bouvier & Del Giorgio, 2007; Thingstad, 2000). Further, protistan grazing on microbial community structures primarily proceed based on cell size-dependent selective predation of prey populations (Jürgens & Matz, 2002; Pernthaler, 2005).

Marine picocyanobacteria mainly comprise *Prochlorococcus* and *Synechococcus*, and are responsible for one-quarter of all global primary production (Falkowski et al., 1998; Flombaum et al., 2013; Partensky et al., 1999). Equally abundant co-occurring cyanophages infect cyanobacteria and significantly shape cyanobacterial population dynamics and their associated organic carbon fluxes in oceans (Biller et al., 2015; Puxty et al., 2016; Sullivan et al., 2003). In addition, ciliates are widespread and abundant phagotrophs in diverse aquatic environments (Calbet & Saiz, 2005; Dziallas et al., 2012). Most ciliates are heterotrophic or mixotrophic protists and important grazers of cyanobacteria, heterotrophic bacteria and other microorganisms (Du Yoo et al., 2015). Together, cyanophage-mediated cyanobacterial lysis and ciliate grazing facilitate the re-mineralization of microbial biomass and promote ecosystem-level nutrient cycling (Fuhrman

& Noble, 1995; Pernthaler, 2005; Sullivan et al., 2003). In addition, microbial interactions between photoautotrophs and heterotrophs, bacteriophage and hosts, and predators and prey, underlie the marine microbial loop and maintain ecosystem stability and community diversity in oceans (Azam et al., 1983; Beliaev et al., 2014; Suttle, 2007). However, the complexity of in situ interaction networks in oceanic environments renders it difficult to evaluate such interactions. Numerous studies have investigated single time-point, seasonal or annual in situ microbial interactions using network analysis (Berdjeb et al., 2011; Chow et al., 2014). Nevertheless, it has remained elusive to confirm the associations between microbial population succession and organic/inorganic nutrient flows associated with top-down controls on microbial food webs in oceans. Furthermore, few studies have evaluated and compared the efficiency of microbial biomass conversion to DOC due to viral lysis and ciliate grazing activities (Haaber & Middelboe, 2009).

Isolated marine unicellular cyanobacterial cultures, including those of *Synechococcus* and *Prochlorococcus*, typically contain co-existing heterotrophic bacterial partners (Cole et al., 2014; Cruz & Neuer, 2019; Moore et al., 2007; Zheng et al., 2018). Thus, cyanobacterial cultures (like *Synechococcus* used in this study) represent useful photoautotroph–heterotroph systems for studying virus-mediated *Synechococcus* lysis and ciliate grazing impacts on the flow of organic and inorganic nutrients, in addition to the functioning of planktonic marine communities in co-culture systems. The aims of the present study were to (i) compare the fluxes of organic matter and inorganic nutrients under virus-mediated *Synechococcus* lysis and *Euplotes* grazing, (ii) characterize the responses and succession of heterotrophic bacterial communities with different lifestyles (free-living vs. attached/aggregated) over time in different treatments and (iii) evaluate the top-down controls impacting the flow of carbon and population dynamics in the *Synechococcus* sp. XM-24 co-culture system.

2 | MATERIALS AND METHODS

2.1 | *Synechococcus*, cyanophage and *Euplotes* grazer cultivation and experimental design

Synechococcus sp. XM-24 and its associated heterotrophic bacterial assemblages were isolated from coastal seawaters at Xiamen Island in China (~24°N, ~118°E) using SN medium (Waterbury, 1986; Zheng et al., 2018). Briefly, the top agar overlay method was used to promote isolation (Brahamsha, 1996). The bottom layer agar concentration was 1.0% (wt/vol), while the top layer concentration was 0.5%. Culture plates were incubated at 25°C under constant cool white fluorescent light illumination (Philips, Somerset, NJ, USA) at 10 $\mu\text{mol photons m}^{-2} \text{s}^{-1}$. *Synechococcus* colonies appeared after 1–2 months of incubation. Single colonies (after 2–3 rounds of purification) were then inoculated into 96-well microtiter plates (Corning, NY, USA), with each well containing 200 μl of SN medium. Co-culture comprised a pure *Synechococcus* strain and

their associated heterotrophic bacterial community that primarily consisted of several dominant bacterial species, as previously described (Zheng et al., 2018). *Synechococcus* strain XM-24 belongs to the 5.2 cyanobacterial subcluster (CB5 clade) that is typically associated with eutrophic estuaries (Chen et al., 2006). The XM-24 co-culture (Figure S1a) comprised a clonal *Synechococcus* strain and diverse heterotrophic bacteria representing a self-selected natural assemblage, in which the dominant heterotrophs could be stably maintained during transfer in liquid medium (Zheng et al., 2018). The heterotrophic bacterial communities associated with the *Synechococcus* sp. XM-24 co-culture were previously investigated, and the 10 most abundant operational taxonomic units (OTUs) comprised >90% of the total heterotrophic community consisting of 380 OTUs (Zheng et al., 2018). Four genomes from the dominant heterotrophic bacterial populations belonging to orders Flavobacteriales, Rhodobacteriales, Cytophagales and Sphingomonadales were previously obtained from metagenomic sequencing and genome binning. The four populations exhibited different lifestyle preferences (free-living vs. attached), metabolic capacities and responses to changes in *Synechococcus* growth phases (Zheng et al., 2019). The XM-24 co-culture (Figure S1a) was incubated at 25°C in SN liquid medium with continuous irradiation at 10 $\mu\text{mol photons m}^{-2} \text{s}^{-1}$ for all experiments in this study.

The *Synechococcus*-associated heterotrophic bacterial populations could be controlled at low abundances after antibiotic treatment (e.g. chloramphenicol, gentamicin) for a short time (3–7 days), as well as using flow cytometer sorting *Synechococcus* cells. However, the populations re-established without continuous addition of antibiotics, precluding the ability to obtain an axenic *Synechococcus* strain. Therefore, the *Synechococcus* strain and its associated natural-selected heterotrophic bacterial assemblages were used as a model photoautotroph–heterotroph system in this study.

The cyanophage SS01 that was used to infect *Synechococcus* sp. XM-24 was isolated from prefiltered (0.22 μm) coastal seawaters around Xiamen Island. The viral particles exhibited icosahedral heads with a diameter of about 55 ± 2 nm and noncontractile tails that were 120 ± 5 nm in length (Figure S1b). The morphological and genomic characteristics of SS01 suggested it was a member of the cyanosiphovirus. The genome sequence of SS01 was deposited in the NCBI database under the BioProject accession PRJNA672221.

The bacterial grazer *Euplotes* (Figure S1c,d) was also isolated from Xiamen area coastal seawaters. *Euplotes* displayed oval or egg morphologies with relatively large sizes of 25–35 \times 40–55 μm (Figure S1c,d). *Euplotes* was chosen as the predator for this study due to the presence of relatively large attached/aggregated cells present in the *Synechococcus* co-culture. *Euplotes* typically feed on bacterial, algal and small protist cells (Dziallas et al., 2012), and are thus an ideal grazer of *Synechococcus* and their associated heterotrophic bacteria. The *Euplotes* culture was maintained at 25°C in sterile-filtered seawater with rice grains. *Euplotes* were selected for the study using a micropipette and a dissecting microscope, followed by washing several times with sterile filtered seawater and scaled up by adding to *Synechococcus* cultures before inoculation.

2.1.1 | Experiment 1

To investigate the influence of cyanophage-mediated *Synechococcus* lysis on the responses of *Synechococcus*-associated heterotrophic bacteria, three batch *Synechococcus* cultures were established in 2-L transparent polycarbonate bottles (Thermo Scientific, Nalgene). Lytic cyanophage was added to the *Synechococcus* culture at day 15 during the middle exponential growth phase of *Synechococcus* with a multiplicity of infection (MOI) value of ~ 0.1 . To eliminate the effects due to adding 100-ml prefiltered (0.22 μm) viral lysates, samples were collected before (i.e. day 15) and after (defined as 15.1) phage addition. No significant ($p < .01$) differences in nutrient concentrations and community composition were detected between these two samples.

2.1.2 | Experiment 2

To investigate the impact of ciliate grazing on the dynamics of *Synechococcus* and their associated heterotrophic bacteria, three batch *Synechococcus* cultures were established in 2-L transparent polycarbonate bottles (Thermo Scientific, Nalgene). The grazer *Euplotes* sp. was added to the *Synechococcus* culture at day seven at an original abundance of 3 cells per ml, which was estimated based on predator-prey relationship dynamics (Figure S2). The ciliate grew slowly in the presence of relatively high *Synechococcus* cell abundances (Figure S2). However, it is difficult to obtain clear patterns of nutrient flows and heterotrophic bacterial responses during viral-mediated lysis when using relatively low *Synechococcus* cell abundances if cyanophage and ciliates are introduced at the same time. Consequently, phage and ciliates were added on different days.

Concomitantly, three batch *Synechococcus* cultures without any additions were incubated as controls in 2-L transparent polycarbonate bottles (Thermo Scientific, Nalgene). To ensure consistent original *Synechococcus* abundances and growth condition, all nine batch *Synechococcus* cultures were inoculated from the same exponential phase *Synechococcus* culture with the initial *Synechococcus* abundance of $\sim 1.60 \times 10^6$ cells per ml. A workflow schematic for the experimental design and data acquisition is shown in Figure S3.

2.2 | Abundances of *Synechococcus*, heterotrophic bacteria and virus-like particles

Synechococcus and heterotrophic bacterial cell numbers within the co-cultures were measured using flow cytometry, as described previously (Zheng et al., 2018). Briefly, an Epics Altra II flow cytometer (Beckman Coulter, Inc., Brea, CA, USA) equipped with an external quantitative sample injector (Harvard Apparatus PHD 2000; Instech Laboratories, Inc.) was used to quantify cells. *Synechococcus* cell numbers were determined from plots of side scatter versus red fluorescence, in addition to plots of orange fluorescence versus red fluorescence (Jiao et al., 2005). Total bacterial cells were enumerated by

staining them with SYBR Green I and using plots of red fluorescence versus green fluorescence and side scatter versus green fluorescence. Subtraction of *Synechococcus* numbers from the total bacterial counts was used to infer heterotrophic bacterial cell abundances. Virus samples were analysed separately from the *Synechococcus* samples. Virus-like particles (VLPs) were discriminated on the basis of green DNA-based SYBR Green I fluorescence versus 90° angle light scatter (Jiao et al., 2005). Flow cytometry data were analysed using the EXPOTM 32 Multi-COMP software program (Beckman Coulter, Inc.).

2.3 | Total organic carbon, DOC and dissolved inorganic nutrient measurements

Liquid culture samples (20 ml) were directly collected into 40-ml glass vials (CNW, Germany) and immediately stored at -20°C for total organic carbon (TOC) analysis. In addition, 20-ml samples were filtered through precombusted (450°C for 4 hr) $0.7\text{-}\mu\text{m}$ pore-size GF/F filters (47 mm diameter, Whatman, Maidstone, UK) into 40-ml glass vials and stored at -20°C for subsequent DOC analysis. TOC and DOC concentrations were measured using high temperature catalytic oxidation on a Shimadzu TOC-VCPH analyzer (Japan) (Sohrin & Sempéré, 2005). Particulate organic carbon (POC) concentrations were measured by subtracting DOC from TOC values. The concentrations of dissolved inorganic nutrients including nitrite, nitrate and phosphate were measured via spectrophotometry, as previously described (Knap et al., 1996) using a Technician AA3 Auto Analyzer (Bran-Lube, GmbH, Germany). Lastly, the indophenol blue method was used to measure ammonium concentrations spectrophotometrically (Ma et al., 2014).

2.4 | Size-fractionated sample harvesting, DNA extractions and 16S rRNA gene sequencing

To collect size-fractionated samples, 50 ml of the liquid cultures was sequentially filtered through 20.0- (only for *Euplotes* addition incubations after day 10), 3.0- and $0.22\text{-}\mu\text{m}$ pore-size polycarbonate filters (47 mm diameter; Millipore, USA) at a vacuum pressure of <0.03 MPa. Filters were flash frozen in liquid nitrogen and stored at -80°C until DNA extraction. DNA was extracted using a hot sodium dodecyl sulphate lysis method with phenol/chloroform extraction, and precipitation with isoamyl alcohol, as previously described (Zheng et al., 2018), followed by storage at -80°C until further use. The quality and quantity of extracted DNA was assessed using a Nano-Drop spectrophotometer (ND-2000; Thermo Fisher).

Extracted DNA from the 134 size-fractionated samples of the *Synechococcus* co-culture incubations was subjected to PCR amplification of 16S rRNA genes using primers targeting the bacterial V3-V4 hypervariable regions (515F, 5'-GTGCCAGCMGCCGCGGTAA-3' and 907R, 5'-CCGTCGAATTCMTTTRAGTTT-3') (Lane, 1991). Sequencing libraries were constructed using the NEBNext® Ultra™ DNA Library

Prep Kit for Illumina (New England Biolabs, USA) according to the manufacturer's recommendations for NEBNext end preparation, adaptor ligation, size selection of adaptor-ligated DNA, PCR enrichment of adaptor-ligated DNA and PCR amplification cleanups. Detailed library construction protocols have been described previously (Zheng et al., 2018). Library quality was assessed using Qubit 2.0 Fluorometer (Thermo Scientific) and Agilent Bioanalyzer 2100 systems. The libraries were then sequenced on the Illumina MiSeq platform with paired-end 250 bp chemistry (Illumina, San Diego, CA, USA). Low quality reads (5-mer $<Q20$, length <150 bp or the presence of ambiguous base-calls) were removed from the library and the remaining paired-end reads were combined using the FLASH software v1.2.7 program (Magoc & Salzberg, 2011). Reads with homopolymer lengths >8 bp or >1 mismatch to the 5' end primer were removed from the libraries using QIIME2 version 2018.4 (Bolyen et al., 2019). Chimeras were then removed with USEARCH v5.2.236 (Edgar et al., 2011). UCLUST was used to cluster the remaining high quality reads into operational taxonomic units (OTUs) at a nucleotide identity cut-off of 97% (Edgar, 2010). OTUs were then taxonomically classified against the RDP database (release 11.1) (Wang et al., 2007) using the QIIME pipeline with default parameters (Bolyen et al., 2019). OTUs with a relative abundance of $<.001\%$ were removed to avoid overestimations of diversity, as described previously (Bokulich et al., 2013). In addition, the reads were also denoised with the deblur algorithm in order to generate amplicon sequence variants (ASVs) (Amir et al., 2017). A total of 6,759,583 paired-end 250-bp read sequences remained after quality control, with between 22,215 and 97,233 sequences for each sample and average sequence lengths of 411 bp. A subset of 21,751 sequences was randomly selected from each sample for further analysis to avoid bias from differential sequencing efforts among samples. The 16S rRNA gene sequence data was deposited in the NCBI Sequence Read Archive under the BioProject accessions PRJNA573984, PRJNA573986 and PRJNA573987.

3 | RESULTS

3.1 | *Synechococcus* co-culture dynamics after cyanophage and *Euplotes* additions

Synechococcus cells were inoculated at a density of $1.58 \pm 0.12 \times 10^6$ cells per ml in all nine incubations, and increased by ~ 60 -fold (reaching $1.01 \pm 0.10 \times 10^8$ cells per ml) at days 22 and 24 in the control group (Figure 1a). Phage was added to the culture at the 15th day of cultivation when *Synechococcus* was in mid-exponential phase ($7.32 \pm 0.38 \times 10^7$ cells per ml) with a MOI value of ~ 0.1 (Figure 1a). The abundance of virus-like particles (VLPs) peaked at $9.21 \pm 1.14 \times 10^8$ VLPs per ml after 30 hr of infection, then quickly decreased by 12-fold (reaching $7.21 \pm 0.24 \times 10^7$ VLPs per ml) at day 17, finally stabilizing at $\sim 2.0 \times 10^7$ VLPs per ml. *Synechococcus* abundances in the phage addition group displayed a 10-fold reduction (ranging from $7.21 \pm 0.54 \times 10^7$ to $6.97 \pm 1.04 \times 10^6$ cells per

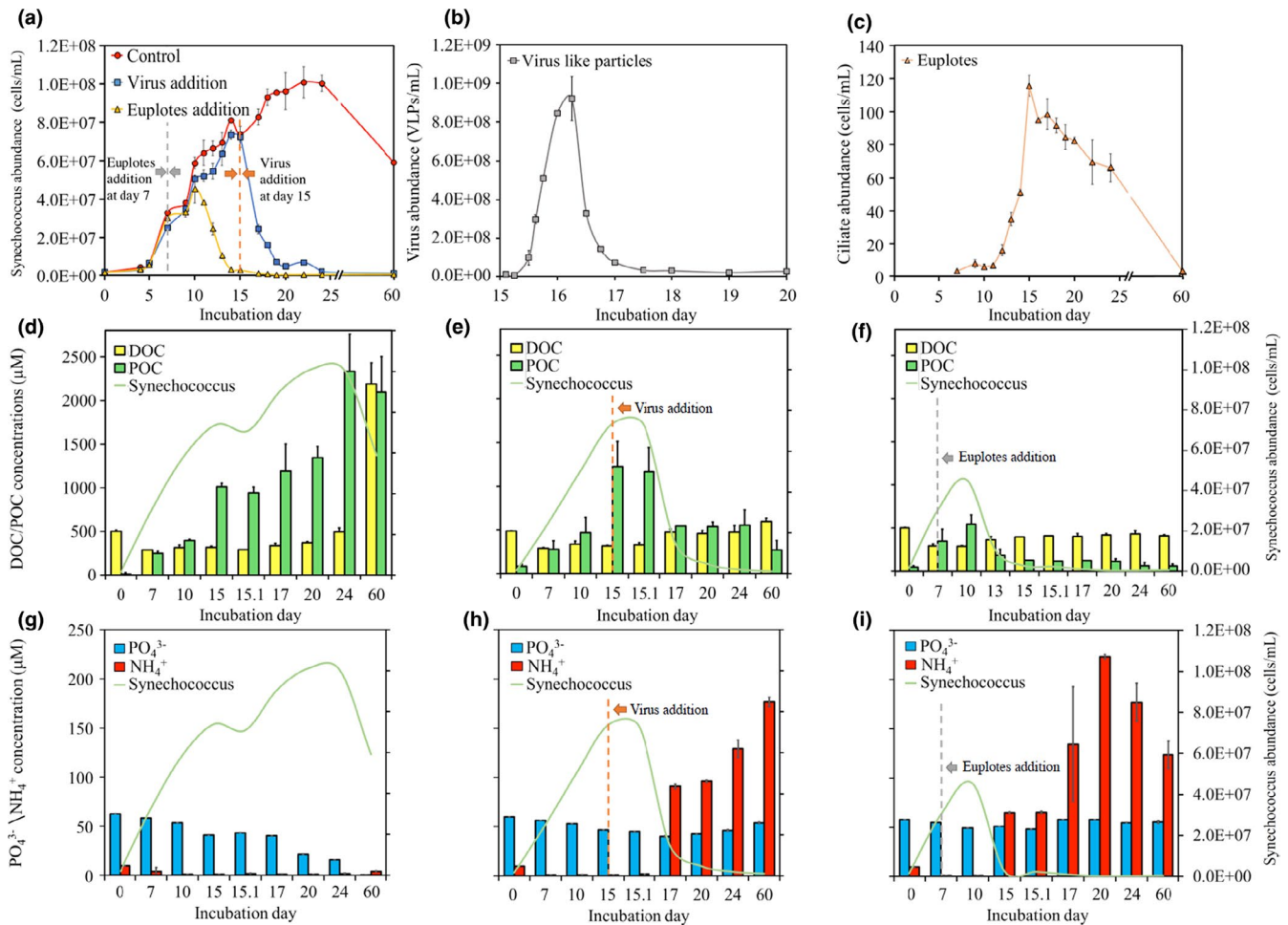


FIGURE 1 Microbial population and organic/inorganic nutrient dynamics over the incubation experiments. The abundances of *Synechococcus* (a) and heterotrophic bacterial (b) cells in control, cyanophage and *Euplotes* treatment groups over the incubations. The abundances of *Euplotes* in ciliate grazing treatment groups (c). DOC and POC concentration dynamics in control (d), cyanophage (e) and *Euplotes* (f) treatment groups, respectively. PO_4^{3-} and NH_4^+ concentrations in control (g), cyanophage (h) and *Euplotes* (i) treatment groups, respectively. The green curves in d–i show the abundances of *Synechococcus* cells, as given by the right Y-axis of the plots. Error bars represent the range of values from duplicate or triplicate measurements. Error bars are not visible when microorganisms were in low abundance due to the unit range used for the Y-axis. PO_4^{3-} concentrations exhibited a wide variation across incubations, although their replicate measurement errors were minimal and are thus not apparent in the graph

ml) between days 15 and 19 and were then maintained at $\sim 5.0 \times 10^6$ cells per ml after day 19 (Figure 1a).

Heterotrophic bacterial abundances increased by 11-fold (from $8.30 \pm 0.22 \times 10^6$ to $9.40 \pm 1.12 \times 10^7$ cells per ml) between days 0 and 15 in both control and treatment groups, and up to 20-fold (peaking at $1.75 \pm 0.11 \times 10^8$ cells per ml) on day 24 in the control group. Heterotrophic bacterial abundances continually increased by 17% (reaching $1.10 \pm 0.16 \times 10^8$ cells per ml on day 17) during the 2-day viral lysis period and were then maintained at $\sim 8.0 \times 10^7$ cells per ml after day 20 in treatment group (Figure 1b).

The grazer *Euplotes* was added to cultures at an original concentration of 3 cells per ml at day 7 when *Synechococcus* abundances were $2.50\text{--}3.30 \times 10^7$ cells per ml (Figure 1a). After an adaptation period between days 7 and 11, *Euplotes* abundances markedly rose by fivefold (from 16 ± 3 to 116 ± 6 cells per ml) during the grazer exponential growth phase (from days 12 to 15) (Figure 1c). After day

16, *Euplotes* abundances slowly declined by 50% (66 ± 8 cells per ml) at day 24. Prior to the 10th day, *Synechococcus* abundances in the ciliate addition group did not exhibit obvious differences with the control group. A sharp 17-fold decline in *Synechococcus* abundances was then observed in the treatment, ranging from $4.53 \pm 0.71 \times 10^7$ to $2.61 \pm 0.14 \times 10^6$ cells per ml which corresponded to the timing of the *Euplotes* exponential growth phase (Figure 1a). *Synechococcus* abundances continually decreased after day 15 to a minimum value of $2.0 \pm 0.68 \times 10^5$ cells per ml at day 19 (Figure 1a). However, a considerable level of attached or aggregated cells primarily comprising heterotrophic bacteria were observed, using fluorescent microscopy and transmission electron microscopy (Figures S4 and S5), especially in the *Euplotes* addition group, rendering it difficult to obtain accurate heterotrophic bacterial cell counts using flow cytometry.

Heterotrophic bacterial abundances increased by fourfold (reaching $4.20 \pm 0.18 \times 10^7$ cells per ml) at day 10 before the *Euplotes*

FIGURE 2 The relative abundances of *Synechococcus* cells (a1–a3) among the total bacterial 16S rRNA sequence data sets and the five dominant heterotrophic bacterial taxa (B, C, D, E AND F) among the total heterotrophic bacterial sequences from the 0.22–3 μm (blue), >3 μm (or 3–20 μm) (yellow) and >20 μm (pink) size fractions over the cultivation experiments in the control (a1–f1), cyanophage (a2–f2) and *Euplotes* (a3–f3) treatment groups, respectively. a, *Synechococcus*, b, *Fluviicola*, c, *Marivita*, d, *Roseivirga*, e, *Altererythrobacter*, f, *Alteromonas*. The green curves show *Synechococcus* abundances in the control (a1–f1) and cyanophage addition (a2–f2) treatment groups, while orange shows the *Euplotes* growth curve. Error bars represent the range of values from two or three biological replicates. Detailed descriptions of the responses of each taxon to viral lysis and *Euplotes* predation is provided in the Supplementary Information

exponential growth phase. Heterotrophic bacterial abundances then decreased by 75% ($9.93 \pm 0.75 \times 10^6$ cells per ml) in conjunction with the highest abundance of *Euplotes* at day 15. Subsequently, heterotrophic bacterial abundances reduced by 98% to its lowest number ($8.66 \pm 1.09 \times 10^5$ cells per ml) at day 24 (Figure 1b).

3.2 | Nutrient variation in the co-culture system

POC concentrations followed *Synechococcus* abundance dynamics in the control group, increasing by 175-fold (from $1.30 \pm 1.01 \times 10^1$ to $2.33 \pm 0.42 \times 10^3$ μM) from the beginning to the 24th day, and decreased slightly by 10% (reaching $2.10 \pm 0.59 \times 10^3$ μM) at the end of the incubations (Figure 1d). DOC concentrations rose by 70% from days 7 to 24 (increasing from $2.89 \pm 0.18 \times 10^2$ to $4.95 \pm 0.45 \times 10^2$ μM) and surpassed POC at day 60 in the decline phase (Figure 1d). Background DOC supported early heterotrophic bacterial growth from the beginning of the experiments to day seven and decreased by 40% (from ~ 500 to ~ 290 μM) over this period. It should be noted that the adaption period would be much longer without addition of organic carbon at the onset of experiments.

After addition of the *Synechococcus* phage, POC concentrations significantly dropped by 50% (from $1.16 \pm 0.27 \times 10^3$ to $5.42 \pm 0.19 \times 10^2$ μM), corresponding to declines in *Synechococcus* abundances between days 15 and 17 (Figure 1e). The DOC concentrations clearly increased by 45% (from $3.26 \pm 0.25 \times 10^2$ to $4.74 \pm 0.34 \times 10^2$ μM) during these two days, and was ~ 140 μM higher than the control group concentrations (Figure 1d,e). The relatively high DOC concentrations in the phage addition group were maintained until day 20.

In the *Euplotes* treatment group, POC concentrations reached a maximum value of $5.45 \pm 1.04 \times 10^2$ μM at day 10 prior to the *Euplotes* exponential growth phase, and then decreased by 66%–76% at days 13 and 15. (Figure 1f). From days 15 to 20, POC concentrations were maintained a relatively stable level (between 1.27×10^2 and $1.14 \pm 0.29 \times 10^2$ μM) (Figure 1f). DOC concentrations increased by 42% (from $2.88 \pm 0.10 \times 10^2$ to $4.08 \pm 0.09 \times 10^2$ μM) during the *Euplotes* exponential growth phase, and then varied minimally (~ 20.0 μM) until the end of the incubation experiments.

Available inorganic phosphate was the primary factor limiting *Synechococcus* growth in the control group, with concentrations varying from 62.6 ± 0.16 to 0.3 ± 0.25 μM over the entire experiment (Figure 1g). However, only a small fraction of inorganic phosphate ($\sim 5\%$ – 10%) was regenerated due to viral lysis and ciliate grazing activities (Figure 1h,i). Ammonium concentrations remained lower than

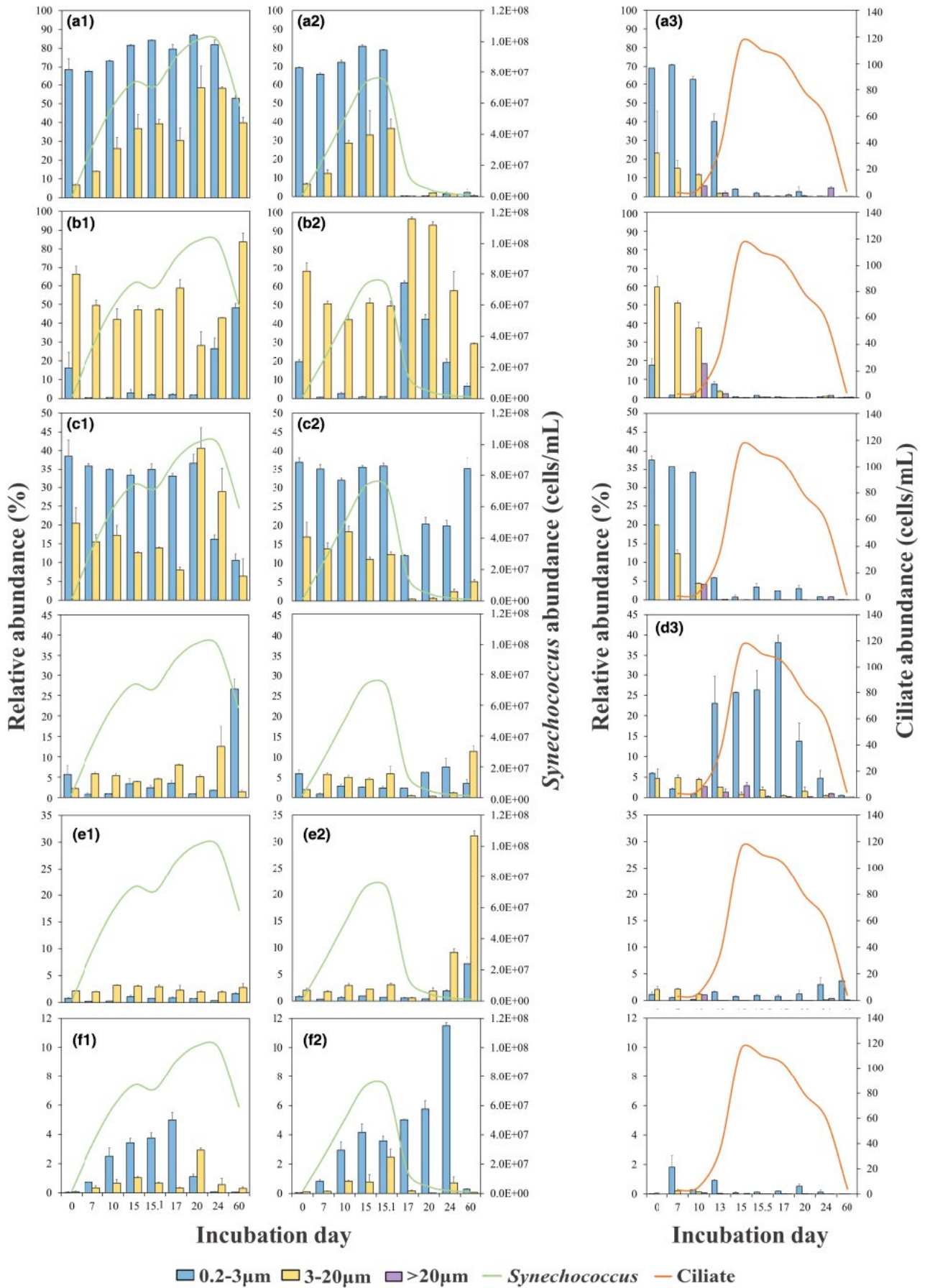
1.5 μM over the entire incubations in the control group, with the exception of the starting (9.6 ± 0.32 μM) and ending (3.9 ± 0.33 μM) days (Figure 1g). In contrast, ammonium concentrations ranged up to 176.7 ± 4.9 and 209.6 ± 85.7 μM in cyanophage and *Euplotes* addition treatments, respectively (Figure 1h,i). The original nitrate concentration was 8 mM in all incubations, and only 25% of the nitrate was used over the entire incubation in the control treatment. Therefore, inorganic nitrogen compounds (primarily nitrate) were abundantly available across the entire incubation period. In the two experimental groups, less than 10% of nitrate was taken up due to the relatively low *Synechococcus* abundances. Furthermore, approximately 5%–8% of nitrate was regenerated due to viral lysis and ciliate predation. The regeneration of phosphate and inorganic nitrogen (especially ammonium) was closely associated with cyanophage-mediated *Synechococcus* lysis and *Euplotes* predation (Figure 1h,i).

3.3 | Microbial assemblages in the incubations

To investigate the responses of different bacterial populations to cyanophage and *Euplotes* treatments in *Synechococcus* cultures, 16S rRNA gene amplicons were sequenced from 134 size-fractionated samples collected throughout the incubations. After subsampling, a total of 2,116,116 bacterial 16S rRNA gene sequences were obtained from 134 samples after removing *Synechococcus* reads. The sequences clustered into 257 OTUs and 480 ASVs, with each abundant OTU primarily comprising one ASV (Table S1). Heterotrophic bacteria were primarily classified to eight orders: Flavobacteriales (relative abundance of 31.2%), Rhodobacterales (23.5%), Saprospirales (15.4%), Rhizobiales (9.6%), Cytophagales (5.7%), Bradymonadales (2.8%), Sphingomonadales (2.5%) and Alteromonadales (2.2%) (Figure S6).

3.3.1 | Responses of *Synechococcus* to cyanophage-induced lysis and *Euplotes* grazing

Synechococcus sp. XM-24 were primarily observed with free-living lifestyles in the control culture over the entire incubation period, and their average relative abundances among the total 16S rRNA sequences were 75.1% and 34.4% within the 0.22–3 and >3 μm size fractions, respectively (Figure 2a1; Figure S6). After phage addition, the relative abundances of *Synechococcus* quickly decreased to less than 0.5% in the two size fractions on day 17 (Figure 2a2). Its relative abundances stabilized at low values (<3%) for both size fractions at the end of



the incubations. *Synechococcus* relative abundances significantly decreased during the *Euplotes* exponential growth phase. Its relative abundances declined by 93.6% (ranging from 62.5% to 3.94%) and 99.3% (ranging from 11.8% to 0.08%) in the 0.22–3 μm and >3 μm size fractions, respectively, from days 10 to 15 (Figure 2a3).

3.3.2 | Responses of *Synechococcus*-associated dominant heterotrophic bacteria to viral lysis and *Euplotes* grazing

The five most abundant bacterial genera comprised more than half of the total heterotrophic bacterial sequences in the control group (Figure 2b1–f1). The five genera corresponded to *Fluviicola*, *Marivita*, *Roseivirga*, *Altererythrobacter* and *Alteromonas* belonging to the orders Flavobacteriales, Rhodobacterales, Cytophagales, Sphingomonadales and Alteromonadales, respectively (Figure S6). Each genus was primarily represented by a specific strain or phylotype (Table S1), and all of the phylotypes corresponded to bacterial taxa with previously recovered genomes, with the exception of *Alteromonas* (Zheng, Lu, et al., 2019).

After cyanophage-mediated *Synechococcus* lysis occurred, the dominant heterotrophic bacterial populations separated from aggregates or association with *Synechococcus* cells and switched lifestyles from attached to free-living (Figure 2b2–f2). This apparent decoupling was particularly observed for the *Fluviicola*, *Marivita*, *Roseivirga* and *Alteromonas* populations (Figure 2b2–d2, 2f2). In addition, both *Fluviicola* and *Alteromonas* populations displayed rapid positive responses to *Synechococcus* lysing, while *Marivita* exhibited an apparent negative response. *Altererythrobacter* did not exhibit immediate growth responses to *Synechococcus* cell lysis due to phage infection, but their abundances increased during later incubation periods.

Dominant heterotrophic bacterial lifestyles also tended to be free-living after the introduction of *Euplotes*, as particularly exemplified by *Roseivirga* and *Altererythrobacter* (Figure 2b3–f3). These results suggest that attached or aggregated bacterial cells were subject to greater predation pressures. Most bacterial species need to enlarge their cells before division, rendering actively growing and abundant bacterial populations highly susceptible to protistan predation and preferential elimination due to larger cell sizes. Such a mechanism could account for the rapid decrease of dominant bacterial populations (e.g. as observed for *Synechococcus*, *Fluviicola* and *Marivita*) in *Synechococcus* cultures after *Euplotes* were introduced. When *Euplotes* were abundant between days 13 to 20, *Roseivirga* relative abundances substantially increased in the free-living size fraction, suggesting that *Roseivirga* may be resistant to *Euplotes* grazing (Figure 2d3).

3.3.3 | The emergence of a ciliate-related zoosphere in *Euplotes* addition incubations

Three size fractions of community samples (0.22–3, 3–20 and >20 μm) were used to investigate the bacterial responses to

Euplotes addition. Some bacterial populations that were not detected or rare in the control and phage addition treatments became dominant in the *Euplotes* addition incubations. These populations comprise what we term the novel ciliate-related zoosphere, and included nine representative genera/groups belonging to nine orders: Rhizobiales (*Maritalea*) (Figure 3a), Bradymonadales (*Bradymonas*) (Figure 3b), Saprospirales (a novel family member, here referred to as Saprospirales sp.) (Figure 3c), Flavobacteriales (*Muricauda*) (Figure 3d), Alteromonadales (*Marinobacter*) (Figure 3e), Cytophagales (*Flexithrix*) (Figure 3f), Thiotrichales (*Francisella*) (Figure 3g), Chromatiales (*Oceanococcus*) (Figure 3h) and Rhodobacterales (*Ponticoccus*) (Figure 3i). Each genus/taxon was primarily represented by one specific strain or phylotype (Table S1), and six of their genomes were also obtained by binning genomes from metagenomes (Table S2, unpublished data).

Overall, bacterial community structure significantly changed in the ciliate addition group relative to the control group, suggesting that the transformation from a *Synechococcus*-driven phycosphere to a *Euplotes*-remodelled zoosphere resulted in whole community-level changes (Figure 3). The zoosphere bacterial communities primarily comprised candidate symbionts (Figure S5M–P) associated with *Euplotes* and grazing-resistant bacterial populations (Figure S4, Figure S5q–x).

3.4 | Top-down controls impact community diversity

Analysis of similarity (ANOSIM) tests revealed that heterotrophic bacterial community structure significantly differed between the 0.22–3 and >3 μm size fractions across the three treatment experiments, as well as between the same size fractions and across different treatment groups (Table S3). However, the microbial communities were highly similar in the 3–20 and the >20 μm size fractions in the *Euplotes* addition treatment (Table S3). Viral lysis and protist grazing could increase or balance diversity in co-cultures and in natural aquatic environments by controlling the abundances of dominant populations (Chow et al., 2014; Weinbauer et al., 2007; Wommack & Colwell, 2000). Viral-mediated *Synechococcus* lysis resulted in slightly increased community richness (based on the Chao1 index) and diversity (based on the Shannon index) (Figure S7a,b). Further, the addition of *Euplotes* grazers significantly ($p < .01$) increased co-culture system richness and diversity (Figure S7a,b). Both the Shannon and richness indices of the >3 μm size fraction communities were significantly higher than those for the 0.22–3 μm fractions in the control communities. However, significant differences in these values were not observed for the cyanophage treatments (Figure S7c,d). Lastly, bacterial diversity in the 0.22–3 μm community size fraction was the highest among the three size fractions in the *Euplotes* addition treatments (Figure S7c,d). The increased diversity in the free-living size fractions likely arose due to rapid growth responses of low abundance bacterial populations (including grazing-resistant populations), increased numbers of bacterial cells

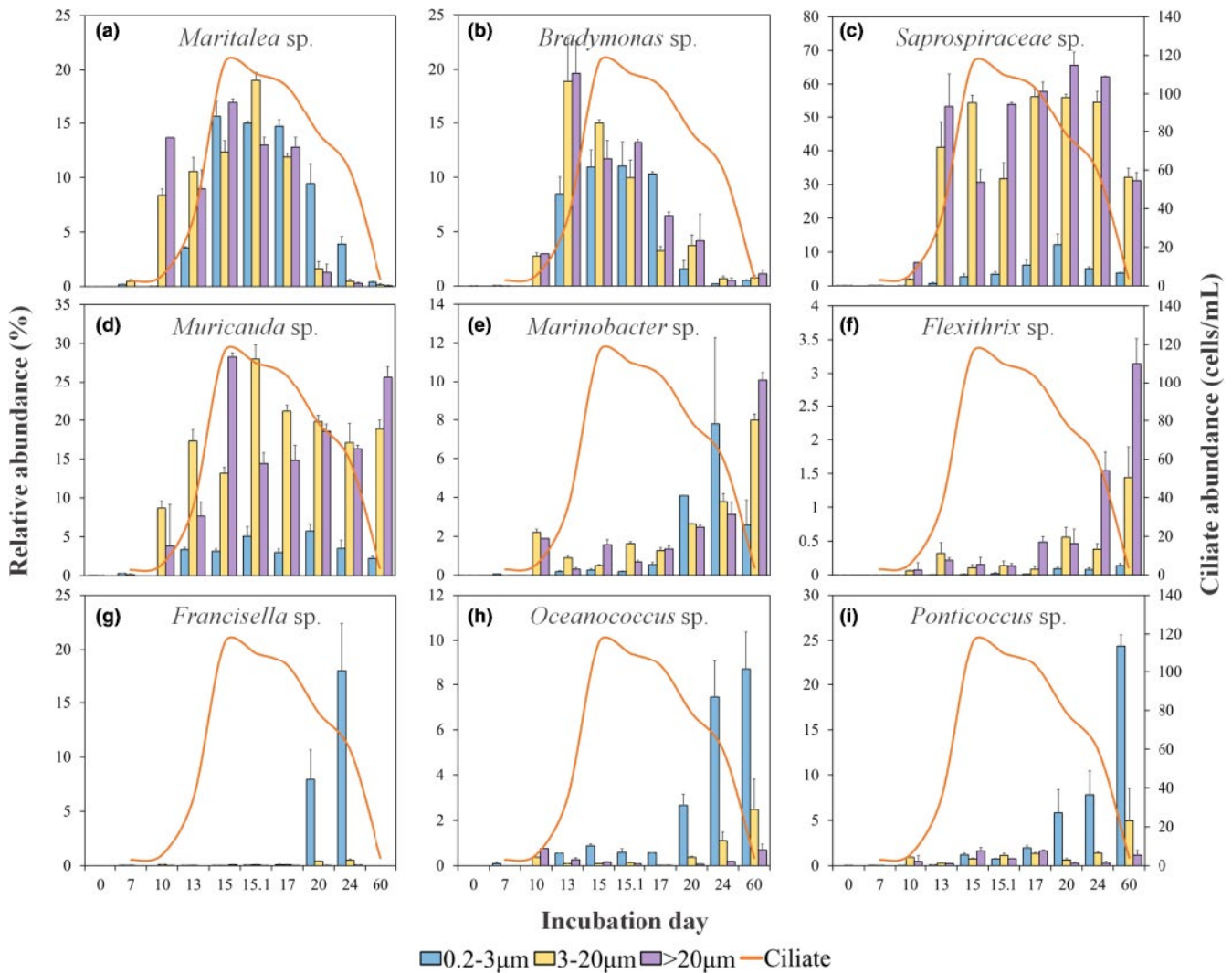


FIGURE 3 The relative abundances of nine dominant heterotrophic bacterial taxa among the total bacterial 16S rRNA sequence data sets in the 0.22–3 μm (blue), 3–20 μm (yellow) and >20 μm (pink) size fractions of the *Euplotes* addition incubations. a, *Maritalea*, b, *Bradymonas*, c, Saprospirales, d, *Muricauda*, e, *Marinobacter*, f, *Flexithrix*, g, *Francisella*, h, *Oceanococcus*, i, *Ponticoccus*. The orange curve shows *Euplotes* abundances over time. Error bars represent the range of values from two or three biological replicates. Detailed descriptions of the responses of each taxon to *Euplotes* predation is provided in the Supplementary Information

separated from attached/aggregated forms, and from contributions to the community of *Euplotes* symbionts in the grazer addition group (Figure 3). In addition, the network analyses based on the ASV-level heterotrophic bacterial species and environmental variables revealed that top-down controls increased co-culture ecosystem complexity, and strengthened microorganism-environment associations (Figure S8).

4 | DISCUSSION

Viral lysis and protist grazing can favour or suppress microbial population growth, with successful bacterial groups being those that survive predation pressure (Perntaler, 2005; Suttle, 2007). Size-fractionation analysis offers an opportunity to investigate shifts

in bacterial populations exhibiting different lifestyles due to lysis or grazing pressure and can also inform phenotypic and genotypic responses of bacterial populations to these top-down control pressures (Figure 4, S4). Viral lysis and protist grazing also facilitate the exchange of bacterial populations between size fractions and were accompanied by the transfer of matter and energy between different microenvironments.

4.1 | Heterotrophic bacterial responses to viral lysis

Cyanophage addition primarily influenced heterotrophic bacterial lifestyles across different size fractions. Four of five dominant populations of the co-culture system (*Fluviicola*, *Marivita*, *Roseivirga* and *Alteromonas*) exhibited obvious decoupling with aggregates or

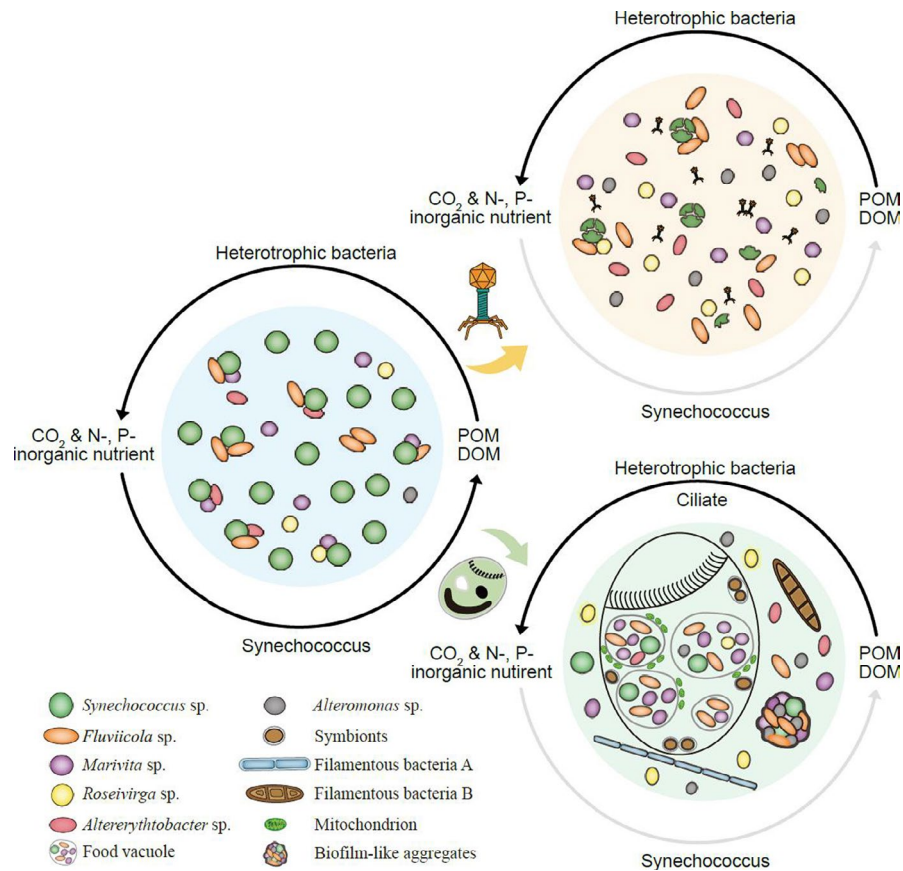


FIGURE 4 Schematic showing variation in nutrient flow and microbial community shifts after cyanophage (above) and *Euplotes* (below) addition into *Synechococcus*–heterotrophic co-culture, respectively. After cyanophage addition, *Fluviicola* and *Alteromonas* displayed a rapid positive response to *Synechococcus* lysates, while *Marivita* exhibited a negative response. *Fluviicola*, *Marivita*, *Roseivirga*, and *Alteromonas* tended to detach from aggregates or with *Synechococcus* cells. In the *Euplotes* addition experiment, the dominant and actively growing bacteria including *Synechococcus*, *Fluviicola* and *Marivita* were highly susceptible to ciliate grazing and were preferentially eliminated by selective grazing pressure in a short time span. Some free-living small bacterial cells with spike-like structures on their cell surfaces could escape *Euplotes* grazing, while other cells (e.g. *Saprospirales*, *Muricauda* and *Flexithrix*) formed filaments or aggregates that become too large to be ingested by the grazer. *Synechococcus* was the only primary producer in the co-cultures and transformed CO₂, N- and P-related inorganic nutrients into organic matter including DOM and POM. Heterotrophic bacteria and ciliates remineralized organic matter to inorganic nutrients, thereby accelerating elemental recycling in the co-culture system

Synechococcus cells. In addition, different heterotrophic bacterial growth responses to virus-mediated *Synechococcus* lysis were apparent. *Fluviicola* and *Alteromonas* exhibited rapid positive growth responses to *Synechococcus* lysing, while *Marivita* exhibited an obvious negative growth response (Figure 2). Polysaccharide utilization loci that encode glycogen utilizing proteins were found in the genomes of the *Fluviicola* and *Alteromonas* strains of the co-culture system (Koch et al., 2019; Zheng, Lu, et al., 2019), indicating their potential close associations with *Synechococcus* and its synthesis of glycogen. In contrast, some cellular components of *Synechococcus* released by lysis or secondary metabolites that were released by bacteria that rapidly responded to the lysis may alternatively constrain *Marivita* growth, explaining its negative response to *Synechococcus* lysis.

Viral lysis likely increased the co-culture system microbial diversity by controlling the abundance of the dominant *Synechococcus* population and supplying organic matter to their associated

heterotrophic bacteria (Chow et al., 2014; Weinbauer et al., 2007; Wommack & Colwell, 2000). Viral-mediated photoautotrophic lysis also likely led to the separation of the associated/symbiotic heterotrophic bacteria from attached cells or aggregates. Consequently, viral-induced lysis might alter the efficiency of the biological carbon pump by allowing DOC to be retained within the euphotic zone (Brussaard et al., 2008; Sheik et al., 2014).

4.2 | The remodelling zoosphere via *Euplotes* addition

All five *Synechococcus*-associated dominant heterotrophic bacterial populations, except *Roseivirga*, quickly exhibited decreased relative abundances after ciliate predation pressure, further transforming the co-culture system from a *Synechococcus*-driven phycosphere to a *Euplotes*-remodelled zoosphere (Figure 4). The zoosphere-influenced

microbial assemblage primarily comprised *Euplotes*-associated symbionts and bacterial populations that were likely grazing-resistant.

4.2.1 | Ciliate-related symbionts

Ciliate cells have been considered as micro-ecosystems that harbour harbouring diverse symbiont communities (Schweikert et al., 2013). *Euplotes* endosymbionts were mostly absent in *Synechococcus* cultures and exhibited variable relative abundances in the different size fractions of the ciliate addition experiments along the ciliate growth phases. For example, *Maritalea* and *Bradymonas* genera were only present in the *Euplotes* addition group communities. These two genera were mainly present in the 3–20 and >20 μm size fractions during the early growth phase of the ciliate, and exhibited rapid increases in relative abundances during the later exponential growth period of the ciliates. Their variation in relative abundances suggested close associations with the growth phases of *Euplotes*. That is, when *Euplotes* performed binary fission in the exponential phase, its endosymbionts also rapidly multiplied. *Maritalea myrionectae* was isolated from a liquid culture of the phototrophic marine ciliate *Myrionecta rubra* during its exponential growth phase (Hwang et al., 2009), further implicating a close and specific association between *Maritalea* and ciliates. The endosymbionts identified in this study were located near the ciliate cell membranes (Figure S5, M–P) and would be easily released into surroundings, thereby displaying free-living lifestyles in the incubations that would become robust during the early stage of ciliate decline. The two bacterial populations could also represent episymbionts. However, no bacterial cells were observed attached to the cell surfaces of *Euplotes* when evaluated with transmission electron microscopy (Figure S5i,m). Most previously studied *Euplotes* endosymbionts have not been able to multiply outside of their hosts, although some pathogenic symbionts (e.g. *Francisella*) have been isolated using specific media (Schrallhammer et al., 2011; Schweikert et al., 2013; Sjödin et al., 2014).

4.2.2 | Grazing-resistant bacterial populations

Size-selective predation has been thoroughly documented in previous studies and is considered an important factor that shapes bacterial community structures in ocean environments (Pernthaler, 2005; Schweikert et al., 2013). Larger bacteria (e.g. those in the >3 μm size fraction) experience higher grazing mortality (Pernthaler, 2005). In contrast, grazing efficiency is relatively low for smaller bacterial cells (e.g. *Roseivirga* sp.), and their relative abundances within microbial assemblages are expected to increase with increasing grazing pressure (Jürgens & Matz, 2002) (Figure 3).

Small free-living bacterial cells can escape protozoan grazing, along with other cells (e.g. Saprospirales, *Muricauda* and *Flexithrix*) by increasing their cell sizes and becoming too large to be ingested by grazers (Figures 3 and 4). The Saprospirales sp. was primarily detected in two large size fractions compared to the free-living

fractions. Further, the relative abundances of the Saprospirales sp. did not vary with *Euplotes* growth phases, remaining relatively stable and abundant throughout the incubations. Members of the closely related Haliscomenobacteraceae family typically grow in thin, barely visible hyaline sheaths that can grow up to dozens of micrometres (Daligault et al., 2011; Van Veen, 1973) and are frequently isolated from phytoplankton cultures (Chen et al., 2014; Lei et al., 2015). *Muricauda*, *Marinobacter*, and *Flexithrix* exhibited similar population dynamics as the Saprospirales sp. Some of the species in these groups have been reported to exhibit long-straight-rod or sheathed-filament morphologies (Arun et al., 2009; Lewin, 1970; Y. Wang et al., 2017). Likewise, the cyanobacterium *Phormidium* sp. resists ciliate grazing by withdrawing inside a polysaccharide envelope and remaining in dense and compact clumps (Fyda et al., 2010). Indeed, bacterial cells commonly form filaments, microcolonies, aggregates and biofilms to protect from predation, wherein cells become embedded in a complex matrix including polysaccharides, proteins, nucleic acids and lipids that can also favour intercellular communication (Jousset, 2012; Salcher et al., 2007). Polysaccharide-rich envelope structures and dense clump-like bacterial aggregates were also frequently detected within our *Euplotes* addition incubations. Similar results have also been observed in environments with high protist grazing, and especially in organic matter-rich incubations (Jürgens & Güde, 1994). Thus, the four bacterial populations identified as being resistant to predation (Saprospirales sp., *Muricauda*, *Marinobacter*, and *Flexithrix*) could potentially represent the long-chain filamentous bacteria and dense aggregates/clumps observed in Figures S4 and S5.

In addition to the above mechanisms, bacterial motility and cell surface structures (e.g. receptor proteins, capsules and exopolymers) can also provide protection against protozoan ingestion or digestion (Pernthaler, 2005). Bacterial cells with spike-like structures on their surfaces were frequently and uniquely found in the *Euplotes* addition incubations (Figure S5w,x). Such structures could be potentially useful in evading grazing. In particular, *Roseivirga* sp. population could be resistant to ciliate grazing via modification of cell surface. Future research could utilize fluorescence in situ hybridization to better link bacterial morphologies, identities and their potential for grazing aversion or endosymbiosis. Nevertheless, the grazing activities of the ciliates likely played significant roles in structuring the size-fraction distribution of heterotrophic bacteria in the co-culture system. Indeed, the incubation system became remodelled from a *Synechococcus*-driven phycosphere to a novel bacterial assemblage that primarily consisted of grazing-resistant bacterial taxa and *Euplotes* symbionts. Importantly, the development of a grazing-resistant bacterial assemblage could lead to slower fluxes of carbon and energy flows via the microbial loop and limit nutrient regeneration (Gong et al., 2016; Jürgens & Güde, 1994).

4.3 | Viral lysis within the aquatic microbial food web

Oceanic cyanophage-host systems are some of the most widely studied and best characterized host-virus model systems (Chow

et al., 2014; Fuhrman & Noble, 1995; Pernthaler, 2005; Sullivan et al., 2003). The addition of phages in our experiments had a pronounced effect on the distribution of organic carbon (DOC vs. POC) due to the transformation of living cells into detritus referred to as lysate. Lysis of *Synechococcus* cells was associated with a dramatic decrease ($\sim 680 \mu\text{M}$) of POC concentrations from within a two-day lysis period (i.e. days 15–17), while DOC concentrations increased by $\sim 140 \mu\text{M}$ during this period, corresponding to a TOC loss of $\sim 540 \mu\text{M}$. These observations indicate that $\sim 80\%$ ($540/680$) of the *Synechococcus* lysates were utilized and respired to CO_2 over a short period of time, suggesting that *Synechococcus*-derived organic matter was mostly labile (Zhao et al., 2019). The relatively high DOC concentration was maintained until day 20 in the cyanophage addition group due to carbon following the 'DOC-bacteria-DOC' loop (Bratbak et al., 1992). During the postlysis period (i.e. days 17–24), both DOC and POC concentrations did not obviously vary. Lysis of the main primary producer in the phage addition group led to the removal of the organic matter source. The result also suggests that phage-mediated lysis of primary producers may be more important than lysis of heterotrophic bacterial cells at the ecosystem level.

Phosphate was the primary factor limiting *Synechococcus* growth in the control group, especially in their stationary and decline growth phases. In addition, phosphate concentrations continuously decreased (from 46.6 to $40.0 \mu\text{M}$) during the viral lysis period. Thus, P-containing organic matter was primarily integrated into heterotrophic bacterial biomass, viral particles, or remained in the original degraded compounds rather than being remineralized into inorganic phosphate during this period. Instead, the regeneration of inorganic phosphate occurred in the postlysis period after day 17. Marine bacteria also accumulate polyphosphate in cells, slowing its cycling within environment (Diaz et al., 2008; Martin et al., 2014). The accumulation of ammonium also corresponded to the utilization of organic matter. A previous incubation experiment also demonstrated that N-containing organic matter from vial lysates can be efficiently remineralized by heterotrophic bacteria, resulting in regenerated ammonium that could then be transferred to phytoplankton (Shelford & Suttle, 2018). In present study, ammonium concentrations quickly increased (from 0.8 to $91.0 \mu\text{M}$) during the viral lysis period, reaching their highest value ($176.7 \mu\text{M}$) at day 60 in the phage addition group. In contrast, ammonium concentrations remained at low values ($<10 \mu\text{M}$) over the entire incubations in the control group. These results indicate that heterotrophic bacteria and *Synechococcus* formed a mutualistic relationship involved in the generation and utilization of ammonium in the control co-culture system (Christie-Oleza et al., 2017). The removal of *Synechococcus* after cyanophage addition directly caused the accumulation of excess ammonium. These results also suggest that the viral shunt is an important component of marine nitrogen biogeochemical cycling, especially in oligotrophic euphotic ocean (Shelford & Suttle, 2018).

Synechococcus lysates comprised highly labile organic matter in our experiments (Zheng, Chen, et al., 2019). Our results indicate that carbohydrates (based on TOC loss) and N-containing lysates were primarily used for energy acquisition by co-cultured cells during

viral lysis and postlysis periods. In contrast, these results point to the P-containing lysates being preferentially used to biosynthesize biomass. In the present study, POC concentrations decreased by $\sim 680 \mu\text{M}$ during the viral lysis period, while DOC quickly increased by $\sim 140 \mu\text{M}$ in the cyanophage addition group relative to the control group. The transfer efficiency from POC to DOC pools was $\sim 20\%$ ($140/680$). DOC comprised heterotrophic bacterial biomass and their secondary metabolites. Based on the conversion of POC and DOC during the *Synechococcus* lysis period, less than 20% of the lysate was converted to bacterial biomass, which is consistent with other reported phytoplankton lysate transfer efficiencies (Haaber & Middelboe, 2009). In addition, varying assimilation efficiencies of phytoplankton viral lysates have been observed for different bacterial species (e.g. *Alteromonas* and *Roseobacter*). Likewise, $\sim 20\%$ of the organic matter derived from the infected *Phaeocystis globosa* cells was transferred to *Alteromonas* sp. cells as based on nano-scale secondary-ion mass spectrometry (Sheik et al., 2014). Furthermore, picophytoplanktonic DOC released by viral lysis comprised 21% of the total carbon production by picophytoplankton in the deep chlorophyll maximum layer of the oligotrophic subtropical north-eastern Atlantic Ocean (Baudoux et al., 2007). Successive utilization of compounds by different bacterial populations transform virus-mediated phytoplankton lysates from labile organic matter to relatively refractory molecules during incubation experiments (Brussaard et al., 2005; Jiao et al., 2010; Zheng, Chen, et al., 2019). The successive regeneration of ammonium and phosphate suggests that the N- and P-containing lysates exhibited different biological availabilities and were likely involved in different microbial metabolic processes. For example, the regeneration of ammonium and phosphate from the degradation of *P. pouchetii* lysates represented 78% and 26% of the lysate N and P, respectively, indicating greater efficiency of heterotrophic N mineralization associated with lysate turnover in the microbial food web relative to P mineralization (Haaber & Middelboe, 2009).

4.4 | Protist grazing as part of the aquatic microbial food web

A previous study of protist grazing indicated that 70% of prey biomass derived from photoautotrophs, while only 30% was from heterotrophic bacteria, indicating that the primary food source available to protists in most regions of the surface ocean was phytoplankton (Ducklow, 2000; Frias-Lopez et al., 2009). Considering that phytoplankton are the main contributors of organic matter to upper oceans, it has been suggested that protistan herbivory of primary producers is more important than bacterivory at the ecosystem level (Sherr & Sherr, 1994). Moreover, protozoan predation of primary producers can affect organic carbon (especially POC) fluxes from the euphotic zone to the dark ocean as a result of feeding selectivity (Sherr & Sherr, 2002).

Ciliate grazing of *Synechococcus* and heterotrophic bacteria are also important components of organic matter redistribution

and inorganic nutrient regeneration in ocean environments. Selective predation by *Euplotes* resulted in low POC concentrations after day 10, including reduction even to the original level (60 μM). DOC concentrations were clearly higher in the ciliate addition group incubations during the exponential and early decline *Euplotes* growth phases (from days 13 to 20) compared to those for the control group. The POC concentration decreased by 418 μM , while the DOC concentration increased by 110 μM during the ciliate rapid growth period from days 10 to 15. The transformation efficiency of POC to DOC was 26% (110/418), also indicating the conversion of microbial biomass to DOC by ciliate grazing activities. Consequently, as much as 74% (308/418) of the organic carbon of the system was respired by *Euplotes* after ingesting bacterial cells, in addition to the contributions from heterotrophic bacterial secondary metabolism. Approximately 73%–81% of the carbon ingested with the bacterial food is estimated to be dissipated through respiration and excretion during predation by two ciliates (*Uronema* and *Euplotes*) (Turley et al., 1986). Other studies have also shown that the addition of ciliate grazers accelerates and enhances the production of new DOC components in laboratory cultures, and the new DOC production during herbivorous grazing represents ~16%–37% of the total algal C content (Kujawinski et al., 2004; Strom et al., 1997). In the aquatic environment, protistan grazing substantially contributes to the decline of phytoplankton blooms. In most cases, only a single protozoan species contributes to these grazing activities, highlighting the importance of specific protist–phytoplankton interactions in aquatic ecosystem (Prakash, 1963; Tillmann, 2004). After peak population growth of *Euplotes*, the microbial communities became ciliate-remodelled zoosphere that contained little or no fresh DOM released by *Synechococcus*. It is likely that these zoosphere bacterial populations are primarily sustained by extracellular DOM production by *Euplotes* (Turley et al., 1986). The impacts of ciliate grazing on different size fractions of bacterial cells and the maintenance of the ciliate-remodelled zoosphere suggests a close interdependence of ciliate predators and their bacterial prey in microbial food webs (Pernthaler, 2005; Turley et al., 1986).

Little variation in phosphate concentrations was observed in the grazing incubations, likely due to the low abundances of *Synechococcus* cells and the concomitant low utilization of phosphate. Only minor variation in phosphate concentrations were observed between days 15 to 17 when phosphate was regenerated (Figure 1i). In contrast, an obvious accumulation of ammonium was observed at day 15 in the grazing treatments, along with a subsequent continuous increase until day 20, ultimately reaching 209.6 μM (Figure 1i). In addition to ammonium accumulation, a significant amount of urea was also released from protistan grazing activities (Saba et al., 2011). These results also suggested that P was mineralized less efficiently than N by the combined effects of ciliate grazing/growth and bacterial secondary metabolism. The accumulation of ammonium was closely associated with the degradation of total organic matter by heterotrophic bacteria and the decay of *Euplotes* cells when *Synechococcus* cells were in low abundance.

5 | CONCLUSION

The forces that regulate bacterial abundances, productivity and community composition is a key area of interest in marine microbial ecology (Jürgens & Matz, 2002). Bottom-up controls and top-down controls are thought to be the primary factors influencing bacterial characteristics in environments (Thingstad & Lignell, 1997; Ward et al., 2013). Phytoplankton are major contributors of labile organic matter to the upper ocean, and heterotrophic bacteria play a central role in the transformation and re-mineralization of these organic matter contents. Here, we evaluated top-down controls on nutrient flows and bacterial responses in a model *Synechococcus*–heterotroph co-culture system. The fractionation of organic matter and regeneration of inorganic nutrients were clearly observed in the cyanophage and ciliate addition experiments. Viral lysis and protozoan grazing increased population diversity by controlling the abundances of the dominant species and causing a preference for free-living bacterial lifestyles. The shift of bacterial lifestyle strategies, succession of different populations and distinct microbial responses to viral lysis and ciliate grazing reflect a highly dynamic co-culture system. Top-down controls on the interactions between photoautotrophs and heterotrophs underlie the marine food web and shape the ecosystem structure and population diversity of the ocean. Further investigation of the combination of bottom-up and top-down control factors will illuminate marine biogeochemistry cycling processes and interaction networks of ocean ecosystems.

ACKNOWLEDGEMENTS

This work was supported by the National Key Research Programs (2018YFA0605800), the Senior User Project of RV KEXUE (KEXUE2019GZ03), the National Natural Science Foundation of China (NSFC) (projects 41776145, 41876150 and 41861144018), the Fundamental Research Funds for the Central Universities (20720190095), and the Natural Science Foundation of Fujian Province of China (2018J05072).

CONFLICTS OF INTEREST

The authors declare that they have no conflicts of interest.

AUTHOR CONTRIBUTIONS

QZ, DX, and NJ conceived and designed the experiments. QZ, WL, YL and YW conducted the experiments. QZ, YW, WL and YL analysed the data. All the authors assisted in writing the manuscript, discussed the results, and commented on the manuscript.

DATA AVAILABILITY STATEMENT

DNA sequences: The 16S rRNA gene sequence data were deposited in the NCBI Sequence Read Archive under the BioProject accessions PRJNA573984, PRJNA573986, and PRJNA573987.

ORCID

Qiang Zheng  <https://orcid.org/0000-0002-6836-2310>

Yu Wang  <https://orcid.org/0000-0001-6100-1312>

REFERENCES

- Amir, A., McDonald, D., Navas-Molina, J. A., Kopylova, E., Morton, J. T., Zech Xu, Z., Kightley, E. P., Thompson, L. R., Hyde, E. R., Gonzalez, A., & Knight, R. (2017). Deblur rapidly resolves single-nucleotide community sequence patterns. *mSystems*, 2(2), <https://doi.org/10.1128/mSystems.00191-16>
- Arun, A., Chen, W.-M., Lai, W.-A., Chao, J.-H., Rekha, P., Shen, F.-T., & Young, C.-C. (2009). *Muricauda lutaonensis* sp. nov., a moderate thermophile isolated from a coastal hot spring. *International Journal of Systematic and Evolutionary Microbiology*, 59(11), 2738–2742.
- Azam, F., Fenchel, T., Field, J., Grey, J., Meyer-Reil, L., & Thingstad, F. (1983). The ecological role of water-column microbes. *Marine Ecology Progress Series*, 10, 257–263.
- Baudoux, A., Veldhuis, M., Noordeloos, A., Van Noort, G., & Brussaard, C. (2008). Estimates of virus-vs. grazing induced mortality of picophytoplankton in the North Sea during summer. *Aquatic Microbial Ecology*, 52(1), 69–82.
- Baudoux, A. C., Veldhuis, M. J. W., Witte, H. J., & Brussaard, C. P. D. (2007). Viruses as mortality agents of picophytoplankton in the deep chlorophyll maximum layer during IRONAGES III. *Limnology and Oceanography*, 52(6), 2519–2529. <https://doi.org/10.4319/lo.2007.52.6.2519>
- Beliaev, A. S., Romine, M. F., Serres, M., Bernstein, H. C., Linggi, B. E., Markillie, L. M., Isern, N. G., Chrisler, W. B., Kucek, L. A., Hill, E. A., Pinchuk, G. E., Bryant, D. A., Steven Wiley, H., Fredrickson, J. K., & Konopka, A. (2014). Inference of interactions in cyanobacterial-heterotrophic co-cultures via transcriptome sequencing. *The ISME Journal*, 8(11), 2243–2255. <https://doi.org/10.1038/ismej.2014.69>
- Berdjeb, L., Pollet, T., Domaizon, I., & Jacquet, S. (2011). Effect of grazers and viruses on bacterial community structure and production in two contrasting trophic lakes. *BMC Microbiology*, 11(1), 88. <https://doi.org/10.1186/1471-2180-11-88>
- Billen, G., Servais, P., & Becquevort, S. (1990). Dynamics of bacterioplankton in oligotrophic and eutrophic aquatic environments: Bottom-up or top-down control? *Hydrobiologia*, 207(1), 37–42. <https://doi.org/10.1007/BF00041438>
- Biller, S. J., Berube, P. M., Lindell, D., & Chisholm, S. W. (2015). Prochlorococcus: The structure and function of collective diversity. *Nature Reviews Microbiology*, 13(1), 13–27. <https://doi.org/10.1038/nrmicro3378>
- Bokulich, N. A., Subramanian, S., Faith, J. J., Gevers, D., Gordon, J. I., Knight, R., Mills, D. A., & Caporaso, J. G. (2013). Quality-filtering vastly improves diversity estimates from Illumina amplicon sequencing. *Nature Methods*, 10(1), 57–59. <https://doi.org/10.1038/nmeth.2276>
- Bolyen, E., Rideout, J. R., Dillon, M. R., Bokulich, N. A., Abnet, C. C., Al-Ghalith, G. A., Alexander, H., Alm, E. J., Arumugam, M., Asnicar, F., Bai, Y., Bisanz, J. E., Bittinger, K., Brejnrod, A., Brislawn, C. J., Brown, C. T., Callahan, B. J., Caraballo-Rodríguez, A. M., Chase, J., ... Caporaso, J. G. (2019). Reproducible, interactive, scalable and extensible microbiome data science using QIIME 2. *Nature Biotechnology*, 37(8), 852–857. <https://doi.org/10.1038/s41587-019-0209-9>
- Boras, J. A., Sala, M. M., Vázquez-Domínguez, E., Weinbauer, M. G., & Vaqué, D. (2009). Annual changes of bacterial mortality due to viruses and protists in an oligotrophic coastal environment (NW Mediterranean). *Environmental Microbiology*, 11(5), 1181–1193. <https://doi.org/10.1111/j.1462-2920.2008.01849.x>
- Bouvier, T., & Del Giorgio, P. (2007). Key role of selective viral-induced mortality in determining marine bacterial community composition. *Environmental Microbiology*, 9(2), 287–297. <https://doi.org/10.1111/j.1462-2920.2006.01137.x>
- Brahmsha, B. (1996). A genetic manipulation system for oceanic cyanobacteria of the genus *Synechococcus*. *Applied and Environmental Microbiology*, 62(5), 1747–1751. <https://doi.org/10.1128/AEM.62.5.1747-1751.1996>
- Bratbak, G., Heldal, M., Thingstad, T., Riemann, B., & Haslund, O. (1992). Incorporation of viruses into the budget of microbial C-transfer. A first approach. *Marine Ecology Progress Series*, 273–280. <https://doi.org/10.3354/meps083273>
- Brussaard, C., Kuipers, B., & Veldhuis, M. (2005). A mesocosm study of *Phaeocystis globosa* population dynamics: I. Regulatory role of viruses in bloom control. *Harmful Algae*, 4(5), 859–874. <https://doi.org/10.1016/j.hal.2004.12.015>
- Brussaard, C. P. D., Wilhelm, S. W., Thingstad, F., Weinbauer, M. G., Bratbak, G., Heldal, M., Kimmance, S. A., Middelboe, M., Nagasaki, K., Paul, J. H., Schroeder, D. C., Suttle, C. A., Vaqué, D., & Wommack, K. E. (2008). Global-scale processes with a nanoscale drive: The role of marine viruses. *ISME Journal*, 2(6), 575–578. <https://doi.org/10.1038/ismej.2008.31>
- Calbet, A., & Saiz, E. (2005). The ciliate-copepod link in marine ecosystems. *Aquatic Microbial Ecology*, 38(2), 157–167. <https://doi.org/10.3354/ame038157>
- Caron, D. A., & Goldman, J. C. (1988). Dynamics of Protistan carbon and nutrient cycling 1, 2. *The Journal of Protozoology*, 35(2), 247–249.
- Chen, F., Wang, K., Kan, J., Suzuki, M. T., & Wommack, K. E. (2006). Diverse and unique picocyanobacteria in Chesapeake Bay, revealed by 16S–23S rRNA internal transcribed spacer sequences. *Applied and Environmental Microbiology*, 72(3), 2239–2243. <https://doi.org/10.1128/AEM.72.3.2239-2243.2006>
- Chen, Z., Lei, X., Lai, Q., Li, Y., Zhang, B., Zhang, J., & Tian, Y. (2014). *Phaeodactylibacter xiamenensis* gen. nov., sp. nov., a member of the family Saprospiraceae isolated from the marine alga *Phaeodactylum tricoratum*. *International Journal of Systematic and Evolutionary Microbiology*, 64(10), 3496–3502.
- Chow, C.-E.-T., Kim, D. Y., Sachdeva, R., Caron, D. A., & Fuhrman, J. A. (2014). Top-down controls on bacterial community structure: Microbial network analysis of bacteria, T4-like viruses and protists. *The ISME Journal*, 8(4), 816. <https://doi.org/10.1038/ismej.2013.199>
- Christie-Oleza, J. A., Sousoni, D., Lloyd, M., Armengaud, J., & Scanlan, D. J. (2017). Nutrient recycling facilitates long-term stability of marine microbial phototroph-heterotroph interactions. *Nature Microbiology*, 2(9), 17100. <https://doi.org/10.1038/nmicrobiol.2017.100>
- Cole, J. K., Hutchison, J. R., Renslow, R. S., Kim, Y.-M., Chrisler, W. B., Engelmann, H. E., Dohnalkova, A. C., Hu, D., Metz, T. O., Fredrickson, J. K., & Lindemann, S. R. (2014). Phototrophic biofilm assembly in microbial-mat-derived unicyanobacterial consortia: Model systems for the study of autotroph-heterotroph interactions. *Frontiers in Microbiology*, 5, 109. <https://doi.org/10.3389/fmicb.2014.00109>
- Cruz, B. N., & Neuer, S. (2019). Heterotrophic bacteria enhance the aggregation of the marine picocyanobacteria *Prochlorococcus* and *Synechococcus*. *Frontiers in Microbiology*, 10, 1864. <https://doi.org/10.3389/fmicb.2019.01864>
- Daligault, H., Lapidus, A., Zeytun, A., Nolan, M., Lucas, S., Del Rio, T. G., Tice, H., Cheng, J.-F., Tapia, R., Han, C., Goodwin, L., Pitluck, S., Liolios, K., Pagani, I., Ivanova, N., Huntemann, M., Mavromatis, K., Mikhailova, N., Pati, A., ... Woyke, T. (2011). Complete genome sequence of *Haliscomenobacter hydrossis* type strain (OT). *Standards in Genomic Sciences*, 4(3), 352. <https://doi.org/10.4056/sigs.1964579>
- Diaz, J., Ingall, E., Benitez-Nelson, C., Paterson, D., de Jonge, M. D., McNulty, I., & Brandes, J. A. (2008). Marine polyphosphate: A key player in geologic phosphorus sequestration. *Science*, 320(5876), 652–655. <https://doi.org/10.1126/science.1151751>
- Dolan, J. R., & Gallegos, C. L. (1991). Trophic coupling of rotifers, microflagellates, and bacteria during fall months in the Rhode River Estuary. *Marine Ecology Progress Series. Oldendorf*, 77(2), 147–156. <https://doi.org/10.3354/meps077147>
- Du Yoo, Y., Seong, K. A., Myung, G., Kim, H. S., Jeong, H. J., Palenik, B., & Yih, W. (2015). Ingestion of the unicellular cyanobacterium *Synechococcus* by the mixotrophic red tide ciliate *Mesodinium rubrum*. *Algae*, 30(4), 281. <https://doi.org/10.4490/algae.2015.30.4.281>

- Ducklow, H. (2000). Bacterial production and biomass in the oceans. *Microbial Ecology of the Oceans*, 1, 85–120.
- Dziallas, C., Allgaier, M., Monaghan, M. T., & Grossart, H.-P. (2012). Act together—implications of symbioses in aquatic ciliates. *Frontiers in Microbiology*, 3, 288. <https://doi.org/10.3389/fmicb.2012.00288>
- Edgar, R. C. (2010). Search and clustering orders of magnitude faster than BLAST. *Bioinformatics*, 26(19), 2460–2461. <https://doi.org/10.1093/bioinformatics/btq461>
- Edgar, R. C., Haas, B. J., Clemente, J. C., Quince, C., & Knight, R. (2011). UCHIME improves sensitivity and speed of chimera detection. *Bioinformatics*, 27(16), 2194–2200. <https://doi.org/10.1093/bioinformatics/btr381>
- Falkowski, P. G., Barber, R. T., & Smetacek, V. (1998). Biogeochemical controls and feedbacks on ocean primary production. *Science*, 281(5374), 200–206.
- Fischer, U. R., Wieltschnig, C., Kirschner, A. K., & Velimirov, B. (2006). Contribution of virus-induced lysis and protozoan grazing to benthic bacterial mortality estimated simultaneously in microcosms. *Environmental Microbiology*, 8(8), 1394–1407. <https://doi.org/10.1111/j.1462-2920.2006.01032.x>
- Flombaum, P., Gallegos, J. L., Gordillo, R. A., Rincon, J., Zabala, L. L., Jiao, N., Karl, D. M., Li, W. K. W., Lomas, M. W., Veneziano, D., Vera, C. S., Vrugt, J. A., & Martiny, A. C. (2013). Present and future global distributions of the marine Cyanobacteria *Prochlorococcus* and *Synechococcus*. *Proceedings of the National Academy of Sciences*, 110(24), 9824–9829. <https://doi.org/10.1073/pnas.1307701110>
- Frias-Lopez, J., Thompson, A., Waldbauer, J., & Chisholm, S. W. (2009). Use of stable isotope-labelled cells to identify active grazers of picocyanobacteria in ocean surface waters. *Environmental Microbiology*, 11(2), 512–525. <https://doi.org/10.1111/j.1462-2920.2008.01793.x>
- Fuhrman, J. A., & Noble, R. T. (1995). Viruses and protists cause similar bacterial mortality in coastal seawater. *Limnology and Oceanography*, 40(7), 1236–1242. <https://doi.org/10.4319/lo.1995.40.7.1236>
- Fyda, J., Fialkowska, E., & Pajdak-Stos, A. (2010). Dynamics of cyanobacteria-ciliate grazer activity in bitrophic and tritrophic microcosms. *Aquatic Microbial Ecology*, 59(1), 45–53. <https://doi.org/10.3354/ame01388>
- Gong, J., Qing, Y., Zou, S. B., Fu, R., Su, L., Zhang, X. L., & Zhang, Q. Q. (2016). Protist-bacteria associations: gammaproteobacteria and alphaproteobacteria are prevalent as digestion-resistant bacteria in ciliated protozoa. *Frontiers in Microbiology*, 7, <https://doi.org/10.3389/fmicb.2016.00498>
- Haaber, J., & Middelboe, M. (2009). Viral lysis of *Phaeocystis pouchetii*: Implications for algal population dynamics and heterotrophic C, N and P cycling. *The ISME Journal*, 3(4), 430. <https://doi.org/10.1038/ismej.2008.125>
- Hutchins, D. A., & Fu, F. (2017). Microorganisms and ocean global change. *Nature Microbiology*, 2(6), 17058. <https://doi.org/10.1038/nrmicrobiol.2017.58>
- Hwang, C. Y., Cho, K. D., Yih, W., & Cho, B. C. (2009). *Maritalea myrionectae* gen. nov., sp. nov., isolated from a culture of the marine ciliate *Myrionecta rubra*. *International Journal of Systematic and Evolutionary Microbiology*, 59, 609–614. <https://doi.org/10.1099/ijs.0.002881-0>
- Jiao, N., Herndl, G. J., Hansell, D. A., Benner, R., Kattner, G., Wilhelm, S. W., Kirchman, D. L., Weinbauer, M. G., Luo, T., Chen, F., & Azam, F. (2010). Microbial production of recalcitrant dissolved organic matter: Long-term carbon storage in the global ocean. *Nature Reviews Microbiology*, 8(8), 593. <https://doi.org/10.1038/nrmicro2386>
- Jiao, N., Yang, Y., Hong, N., Ma, Y., Harada, S., Koshikawa, H., & Watanabe, M. (2005). Dynamics of autotrophic picoplankton and heterotrophic bacteria in the East China Sea. *Continental Shelf Research*, 25(10), 1265–1279. <https://doi.org/10.1016/j.csr.2005.01.002>
- Jousset, A. (2012). Ecological and evolutive implications of bacterial defences against predators. *Environmental Microbiology*, 14(8), 1830–1843. <https://doi.org/10.1111/j.1462-2920.2011.02627.x>
- Jürgens, K., & Güde, H. (1994). The potential importance of grazing-resistant bacteria in planktonic systems. *Marine Ecology Progress Series*, 169–188. <https://doi.org/10.3354/meps112169>
- Jürgens, K., & Matz, C. (2002). Predation as a shaping force for the phenotypic and genotypic composition of planktonic bacteria. *Antonie Van Leeuwenhoek*, 81(1–4), 413–434.
- Knap, A., Michaels, A., Close, A., Ducklow, H., & Dickson, A. (Eds.) (1996). Protocols for the joint global ocean flux study (JGOFS) core measurements. JGOFS Report Nr. 19, 170 pp. Reprint of the IOC Manuals and Guides No. 29, UNESCO, 1994.
- Koch, H., Dürwald, A., Schweder, T., Noriega-Ortega, B., Vidal-Melgosa, S., Hehemann, J.-H., Dittmar, T., Freese, H. M., Becher, D., Simon, M., & Wietz, M. (2019). Biphasic cellular adaptations and ecological implications of *Alteromonas macleodii* degrading a mixture of algal polysaccharides. *ISME Journal*, 13(1), 92–103. <https://doi.org/10.1038/s41396-018-0252-4>
- Kujawinski, E. B., Del Vecchio, R., Blough, N. V., Klein, G. C., & Marshall, A. G. (2004). Probing molecular-level transformations of dissolved organic matter: Insights on photochemical degradation and protozoan modification of DOM from electrospray ionization Fourier transform ion cyclotron resonance mass spectrometry. *Marine Chemistry*, 92(1–4), 23–37. <https://doi.org/10.1016/j.marchem.2004.06.038>
- Lane, D. J. (1991) 16S/23S rRNA Sequencing. In E. Stackebrandt & M. Goodfellow (Eds.), *Nucleic acid techniques in bacterial systematics* (pp. 115–175). John Wiley and Sons.
- Lei, X., Li, Y. I., Wang, G., Chen, Y., Lai, Q., Chen, Z., Zhang, J., Liao, P., Zhu, H., Zheng, W., & Zheng, T. (2015). *Phaeodactylibacter luteus* sp. nov., isolated from the oleaginous microalga *Picochlorum* sp. *International Journal of Systematic and Evolutionary Microbiology*, 65(8), 2666–2670. <https://doi.org/10.1099/ijs.0.000321>
- Lewin, R. A. (1970). *Flexithrix dorotheae* gen. et sp. nov. (Flexibacterales); and suggestions for reclassifying sheathed bacteria. *Canadian Journal of Microbiology*, 16(6), 511–515.
- Ma, J., Adornato, L., Byrne, R. H., & Yuan, D. (2014). Determination of nanomolar levels of nutrients in seawater. *TrAC Trends in Analytical Chemistry*, 60, 1–15. <https://doi.org/10.1016/j.trac.2014.04.013>
- Magoc, T., & Salzberg, S. L. (2011). FLASH: Fast length adjustment of short reads to improve genome assemblies. *Bioinformatics*, 27(21), 2957–2963. <https://doi.org/10.1093/bioinformatics/btr507>
- Martin, P., Dyhrman, S. T., Lomas, M. W., Poulton, N. J., & Van Mooy, B. A. S. (2014). Accumulation and enhanced cycling of polyphosphate by Sargasso Sea plankton in response to low phosphorus. *Proceedings of the National Academy of Sciences of the United States of America*, 111(22), 8089–8094. <https://doi.org/10.1073/pnas.1321719111>
- Moore, L. R., Coe, A., Zinser, E. R., Saito, M. A., Sullivan, M. B., Lindell, D., & Chisholm, S. W. (2007). Culturing the marine cyanobacterium *Prochlorococcus*. *Limnology and Oceanography: Methods*, 5(10), 353–362.
- Morán, X. A. G., Gasol, J. M., Pernice, M. C., Mangot, J.-F., Massana, R., Lara, E., Vaqué, D., & Duarte, C. M. (2017). Temperature regulation of marine heterotrophic prokaryotes increases latitudinally as a breach between bottom-up and top-down controls. *Global Change Biology*, 23(9), 3956–3964. <https://doi.org/10.1111/gcb.13730>
- Partensky, F., Hess, W. R., & Vaulot, D. (1999). *Prochlorococcus*, a marine photosynthetic prokaryote of global significance. *Microbiology and Molecular Biology Reviews*, 63(1), 106–127. <https://doi.org/10.1128/MMBR.63.1.106-127.1999>
- Perntaler, J. (2005). Predation on prokaryotes in the water column and its ecological implications. *Nature Reviews Microbiology*, 3(7), 537. <https://doi.org/10.1038/nrmicro1180>
- Prakash, A. (1963). Source of paralytic shellfish toxin in the Bay of Fundy. *Journal of the Fisheries Board of Canada*, 20(4), 983–996.
- Puxty, R. J., Millard, A. D., Evans, D. J., & Scanlan, D. J. (2016). Viruses inhibit CO₂ fixation in the most abundant phototrophs on earth.

- Current Biology*, 26(12), 1585–1589. <https://doi.org/10.1016/j.cub.2016.04.036>
- Saba, G. K., Steinberg, D. K., & Bronk, D. A. (2011). The relative importance of sloppy feeding, excretion, and fecal pellet leaching in the release of dissolved carbon and nitrogen by *Acartia tonsa* copepods. *Journal of Experimental Marine Biology and Ecology*, 404(1–2), 47–56. <https://doi.org/10.1016/j.jembe.2011.04.013>
- Salcher, M. M., Hofer, J., Horňák, K., Jezbera, J., Sonntag, B., Vrba, J., & Posch, T. (2007). Modulation of microbial predator-prey dynamics by phosphorus availability: Growth patterns and survival strategies of bacterial phylogenetic clades. *FEMS Microbiology Ecology*, 60(1), 40–50.
- Schrallhammer, M., Schweikert, M., Vallesi, A., Verni, F., & Petroni, G. (2011). Detection of a novel subspecies of *Francisella noatunensis* as endosymbiont of the ciliate *Euplotes raikovi*. *Microbial Ecology*, 61(2), 455–464. <https://doi.org/10.1007/s00248-010-9772-9>
- Schweikert, M., Fujishima, M., & Görtz, H.-D.-J.-T. (2013). Symbiotic associations between ciliates and prokaryotes. In E. Rosenberg, E. F. DeLong, S. Lory, E. Stackebrandt, & F. Thompson (Eds.), *The Prokaryotes*. Springer.
- Sheik, A. R., Brussaard, C. P. D., Lavik, G., Lam, P., Musat, N., Krupke, A., Littmann, S., Strous, M., & Kuypers, M. M. M. (2014). Responses of the coastal bacterial community to viral infection of the algae *Phaeocystis globosa*. *ISME Journal*, 8(1), 212–225. <https://doi.org/10.1038/ismej.2013.135>
- Shelford, E. J., & Suttle, C. A. (2018). Virus-mediated transfer of nitrogen from heterotrophic bacteria to phytoplankton. *Biogeosciences*, 15(3), 809–819. <https://doi.org/10.5194/bg-15-809-2018>
- Sherr, E. B., & Sherr, B. F. (1994). Bacterivory and herbivory: Key roles of phagotrophic protists in pelagic food webs. *Microbial Ecology*, 28(2), 223–235. <https://doi.org/10.1007/BF00166812>
- Sherr, E. B., & Sherr, B. F. (2002). Significance of predation by protists in aquatic microbial food webs. *Antonie Van Leeuwenhoek*, 81(1–4), 293–308.
- Sjodin, A., Ohrman, C., Backman, S., Larkeryd, A., Granberg, M., Lundmark, E., Karlsson, E., Nilsson, E., Vallesi, A., Tellgren-Roth, C., Stenberg, P., & Theläus, J. (2014). Complete genome sequence of *Francisella endociliophora* strain FSC1006, isolated from a laboratory culture of the marine ciliate *Euplotes raikovi*. *Genome Announcements*, 2(6), <https://doi.org/10.1128/genomeA.01227-14>
- Sohrin, R., & Sempéré, R. (2005). Seasonal variation in total organic carbon in the northeast Atlantic in 2000–2001. *Journal of Geophysical Research: Oceans*, 110(C10).
- Strom, S. L., Benner, R., Ziegler, S., & Dagg, M. J. (1997). Planktonic grazers are a potentially important source of marine dissolved organic carbon. *Limnology and Oceanography*, 42(6), 1364–1374. <https://doi.org/10.4319/lo.1997.42.6.1364>
- Sullivan, M. B., Waterbury, J. B., & Chisholm, S. W. (2003). Cyanophages infecting the oceanic cyanobacterium *Prochlorococcus*. *Nature*, 424(6952), 1047. <https://doi.org/10.1038/nature01929>
- Suttle, C. A. (2007). Marine viruses—major players in the global ecosystem. *Nature Reviews Microbiology*, 5(10), 801. <https://doi.org/10.1038/nrmicro1750>
- Talmy, D., Beckett, S. J., Zhang, A. B., Taniguchi, D. A., Weitz, J. S., & Follows, M. J. (2019). Contrasting controls on microzooplankton grazing and viral infection of microbial prey. *Frontiers in Marine Science*, 6, <https://doi.org/10.3389/fmars.2019.00182>
- Thingstad, T. F. (2000). Elements of a theory for the mechanisms controlling abundance, diversity, and biogeochemical role of lytic bacterial viruses in aquatic systems. *Limnology and Oceanography*, 45(6), 1320–1328. <https://doi.org/10.4319/lo.2000.45.6.1320>
- Thingstad, T. F., & Lignell, R. (1997). Theoretical models for the control of bacterial growth rate, abundance, diversity and carbon demand. *Aquatic Microbial Ecology*, 13(1), 19–27. <https://doi.org/10.3354/ame013019>
- Tillmann, U. (2004). Interactions between planktonic microalgae and protozoan grazers. *Journal of eukaryotic microbiology*, 51(2), 156–168.
- Turley, C. M., Newell, R. C., & Robins, D. B. (1986). Survival strategies of two small marine ciliates and their role in regulating bacterial community structure under experimental conditions. *Marine Ecology Progress Series*, 33(1), 59–70. <https://doi.org/10.3354/meps033059>
- Van Veen, W. (1973). Bacteriology of activated sludge, in particular the filamentous bacteria. *Antonie Van Leeuwenhoek*, 39(1), 189–205. <https://doi.org/10.1007/BF02578852>
- Wang, Q., Garrity, G. M., Tiedje, J. M., & Cole, J. R. (2007). Naïve Bayesian classifier for rapid assignment of rRNA sequences into the new bacterial taxonomy. *Applied and Environmental Microbiology*, 73(16), 5261–5267.
- Wang, Y., Yang, X., Liu, J., Wu, Y., & Zhang, X.-H. (2017). *Muricauda lutea* sp. nov., isolated from seawater. *International Journal of Systematic and Evolutionary Microbiology*, 67(4), 1064–1069. <https://doi.org/10.1099/ijsem.0.001792>
- Ward, B. A., Dutkiewicz, S., & Follows, M. J. (2013). Modelling spatial and temporal patterns in size-structured marine plankton communities: Top-down and bottom-up controls. *Journal of Plankton Research*, 36(1), 31–47. <https://doi.org/10.1093/plankt/fbt097>
- Waterbury, J. B. (1986). Biological and ecological characterization of the marine unicellular cyanobacterium *Synechococcus*. *Photosynthetic Picoplankton*, 71–120.
- Weinbauer, M. G., Hornák, K., Jezbera, J., Nedoma, J., Dolan, J. R., & Šimek, K. (2007). Synergistic and antagonistic effects of viral lysis and protistan grazing on bacterial biomass, production and diversity. *Environmental Microbiology*, 9(3), 777–788. <https://doi.org/10.1111/j.1462-2920.2006.01200.x>
- Wommack, K. E., & Colwell, R. R. (2000). Virioplankton: Viruses in aquatic ecosystems. *Microbiology and Molecular Biology Reviews*, 64(1), 69–114. <https://doi.org/10.1128/MMBR.64.1.69-114.2000>
- Worden, A. Z., & Binder, B. J. (2003). Application of dilution experiments for measuring growth and mortality rates among *Prochlorococcus* and *Synechococcus* populations in oligotrophic environments. *Aquatic Microbial Ecology*, 30(2), 159–174. <https://doi.org/10.3354/ame030159>
- Zhao, Z., Gonsior, M., Schmitt-Kopplin, P., Zhan, Y. C., Zhang, R., Jiao, N. Z., & Chen, F. (2019). Microbial transformation of virus-induced dissolved organic matter from picocyanobacteria: Coupling of bacterial diversity and DOM chemodiversity. *ISME Journal*, 13(10), 2551–2565. <https://doi.org/10.1038/s41396-019-0449-1>
- Zheng, Q., Chen, Q., Cai, R., He, C., Guo, W., Wang, Y., & Jiao, N. (2019). Molecular characteristics of microbially mediated transformations of *Synechococcus*-derived dissolved organic matter as revealed by incubation experiments. *Environmental Microbiology*.
- Zheng, Q., Lu, J., Wang, Y., & Jiao, N. (2019). Genomic reconstructions and potential metabolic strategies of generalist and specialist heterotrophic bacteria associated with an estuary *Synechococcus* culture. *FEMS Microbiology Ecology*, 95(3), fuz017.
- Zheng, Q., Wang, Y., Xie, R., Lang, A. S., Liu, Y., Lu, J., & Jiao, N. (2018). Dynamics of heterotrophic bacterial assemblages within *Synechococcus* cultures. *Applied and Environmental Microbiology*, 84(3), e01517-01517.

SUPPORTING INFORMATION

Additional supporting information may be found online in the Supporting Information section.

How to cite this article: Zheng Q, Lin W, Wang Y, Xu D, Liu Y, Jiao N. Top-down controls on nutrient cycling and population dynamics in a model estuarine photoautotroph-heterotroph co-culture system. *Mol Ecol*. 2020;00:1–16. <https://doi.org/10.1111/mec.15750>